Apparatus for the measurement of the magnetic susceptibility of liquids in high magnetic fields

J. S. Brooks and G. O. Zimmerman

Boston University, Boston, Massachusetts 02215

R. Meservey

Francis Bitter National Magnet Laboratory, MIT, Cambridge, Massachusetts 02139

(Received 4 April 1983; accepted for publication 9 May 1983)

We describe an apparatus capable of measuring the magnetic force on small liquid samples in high magnetic fields. The apparatus has been used to measure the magnetic susceptibility χ of liquid He at pressures up to 3 MPa in high magnetic fields and has a sensitivity in such measurements comparable to superconducting magnetometers in lower fields. The performance was tested by measuring the atomic diamagnetism of liquid ^{4}He and liquid ^{3}He as well as the nuclear paramagnetism of liquid ^{3}He at 1.2 K in fields up to 15 T.

PACS numbers: 07.55. + x, 75.30.Cr, 67.90. + z

INTRODUCTION

Magnetometry has been reviewed recently by Foner,[1] who discussed the suitability of a magnetometer to its environment. We are interested in the properties of liquid and solid ^{3}He at low temperatures and in high magnetic fields. These constraints demand an apparatus which can withstand internal pressures of up to 5 MPa, operate in a small space, and maintain high stability with varying temperature. In addition, high sensitivity ($\Delta\chi \simeq 10^{-12}$ emu/g) and the ability to operate in intense and noisy magnetic fields is required. In this article we describe an apparatus designed to meet these requirements, and report measurements with pressurized liquid helium using the apparatus. An apparatus to measure the susceptibility of liquid helium at the saturated vapor pressure has been previously reported.[2]

I. THEORY OF OPERATION

A material of uniform magnetic susceptibility χ per unit volume in a magnetic field gradient experiences a force per unit volume given (in rationalized mks units[3]) by

$$\mathbf{f} = -\frac{\chi}{\mu_0}\nabla(B^2/2). \tag{1}$$

If the material is in the form of a cylinder of uniform cross-sectional area A, the magnitude of the net force F in the axial direction on the cylinder whose ends are at positions x_1 and x_2 is

$$F = -\frac{A\chi}{\mu_0}\int_{x_1}^{x_2}\nabla(B^2/2)d\mathbf{x} = -\frac{A\chi}{\mu_0}\int_{B_1}^{B_2} d(B^2/2). \tag{2}$$

This net force in the axial direction can thus be written in terms of the values of the magnetic field at each end of the cylinder:

$$F = -\frac{A\chi}{2\mu_0}(B_2^2 - B_1^2). \tag{3}$$

This is just the usual equation for the Gouy balance[4] and in the present apparatus the same principle is employed, but in a way adapted to our measurements.

II. EXPERIMENTAL APPARATUS

Figure 1 shows the design of the sample chamber assembly. The sample chamber S and the empty compensating chamber S′ are made of quartz tubing. Quartz and optical flats F and F′, metallized with sputtered molybdenum, are positioned parallel with a 25-μm separation and form a capacitor. The sample chamber is filled through the quartz capillary tube T which also provides the restoring force of the force balance. A quartz-to-copper housekeeper seal H is the transition from the quartz to a stainless-steel capillary leading to a high-pressure gas supply at room temperature.

The small space required of any low-temperature apparatus makes it necessary to produce a significant field gradient over a small region of the sample, whose length is typically 1 cm or less. This is accomplished by positioning a small hollow ferromagnetic cylinder in the central, homogeneous region of a Bitter solenoid magnet with its axis parallel to the applied field. Provided the applied field is much greater than that required to effectively saturate the ferromagnet, the difference ΔB between the field B along the axis and the applied

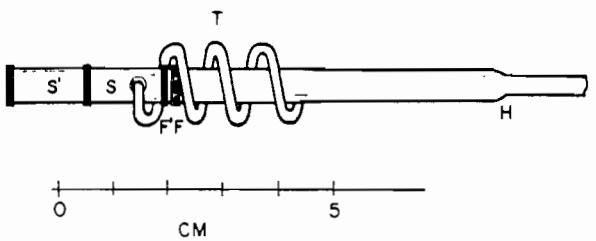

FIG. 1. Schematic diagram of the quartz apparatus showing the sample chamber S, the compensating chamber S′, the metallized optical flats F, F′ forming the capacitor, the quartz spiral tube T, and the glass-to-metal seal H.

field B_0 is given by

$$\Delta B = \frac{\mu_0 M_s}{2}\left[(x-c)\left(+\frac{1}{\sqrt{(x-c)^2+a^2}} - \frac{1}{\sqrt{(x-c)^2+b^2}}\right) - (x+c)\left(+\frac{1}{\sqrt{(x+c)^2+a^2}} - \frac{1}{\sqrt{(x+c)^2+b^2}}\right)\right]. \quad (4)$$

Here the positive sign of the square root is assumed and a, b, c, and x are defined in Fig. 2. In this figure the sample and compensating chambers are drawn to scale with the hollow iron cylinder. Superimposed is the shielding function ΔB as a function of distance x along the axis for the iron cylinder used (saturation magnetic moment $\mu_0 M_s = 2.2$ T) of the proportions shown. Equation (4) provides a simple and reasonably accurate method of calculating the force on the sample. For a more exact calculation which considers the off-axis field, numerical evaluation by computer can be used, but is unnecesary for the basic design calculation.

Although a perfectly symmetrical instrument would only respond when a sample is present, this is not true in practice. Figure 3 schematically shows the instrument, an axial variation of the applied field, and the shielding function to illustrate the effect of asymmetry of the sample chamber with respect to the iron cylinder and displacement of the instrument from the center of the magnet. Some asymmetry is inherent in the instrument because the capillary tube attached to the sample chamber is not matched with a tube attached to the compensating chamber. However, the effect of this asymmetry is rather small because there is little magnetic field gradient in the region of the capillary. Assuming that the center of the instrument is displaced as shown from the center of the iron cylinder and from the center of the magnet, we can calculate the force on the sample and on the quartz cell when empty. Assuming that the sample susceptibility χ_s and the sample chamber susceptibility χ_q are both constant and have constant cross sections, we can use Eq. (3) to calculate the forces. Equation (5) gives the force on the sample and Eq. (6) gives the force on the quartz sample chamber:

$$F_s = \frac{\chi_s A_s}{2\mu_0}\{[B_0(1+\alpha)+\Delta b_a]^2 - [B_0+\Delta b_0]^2\}, \quad (5)$$

$$F_q = \frac{\chi_q A_q}{2\mu_0}\{[B_0(1+\alpha)+\Delta b_a]^2 - [B_0(1+\beta)+\Delta b_b]^2\}. \quad (6)$$

Expanding Eqs. (5) and (6) and neglecting higher-order terms,

$$F_s = \frac{\chi_s A_s}{\mu_0}[aB_0^2 + (\Delta b_a - \Delta b_0)B_0], \quad (5a)$$

$$F_q = \frac{\chi_q A_q}{\mu_0}[(\alpha-\beta)B_0^2 + (\Delta b_a - \Delta b_b)B_0]. \quad (6a)$$

From Eq. (5a) we see that when $\alpha = 0$, which means that the applied field is uniform or at least the same at points 0, and a, F_s is proportional to χ_s and B_0:

$$F_s \sim \chi_s A_s(\Delta B_a - \Delta B_0)B_0. \quad (7)$$

If, on the other hand, $\alpha \neq 0$, F_s will have a term in B_0^2. The background term acting on the sample chamber will also have a linear term from the iron shielding cylinder and a quadratic term from the asymmetry of the applied field. In our experience it turns out that the force on the sample is nearly linear in B_0 while the background term for an empty cell is mainly quadratic.

The force F_s on a liquid-helium sample in our apparatus at 10 T is about 5×10^{-5} N. The force is measured through the change in capacitance C caused by the extension or compression of the quartz capillary spring. The extension of the end of the spiral capillary in the axial direction (which is also the displacement of the sample chamber) is related to the

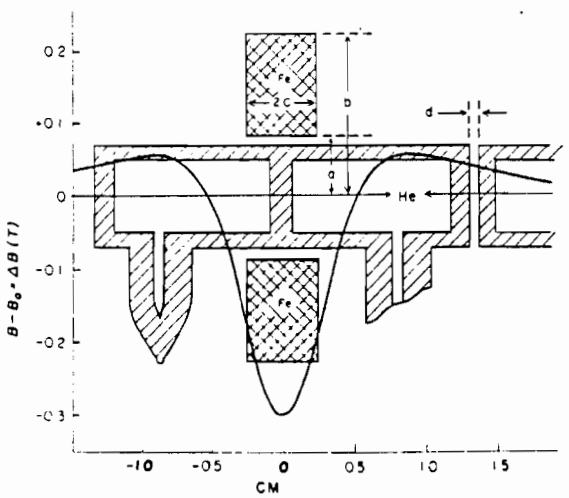

FIG. 2. Quartz force balance showing the sample and compensating chambers, the fill capillary, the capacitance transducer, and the iron cylinder. The shielding function of the iron cylinder in a high magnetic field is also shown. Dimensions of the iron cylinder are $a = 0.42$ cm, $b = 1.14$ cm, and $2c = 0.508$ cm, and dimensions of the quartz are approximately to scale. The separation of the capacitor plates $d = 25\ \mu$m.

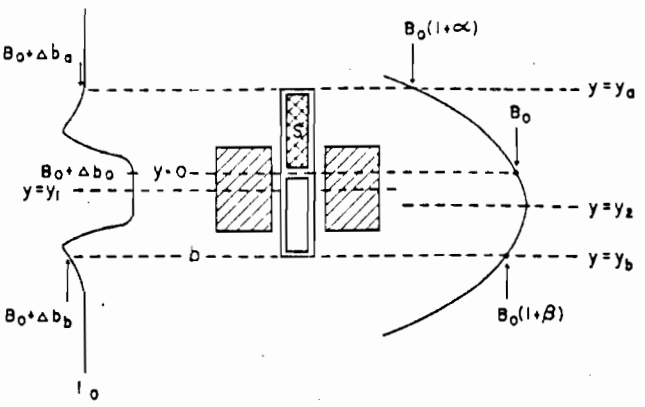

FIG. 3. Schematic diagram showing an unsymmetrical placement of the sample cell S with respect to the iron cylinder and with a displacement of the instrument from the center of the magnet. The effect of these asymmetries on the response both full and empty is discussed in the text.

applied force F by

$$\Delta x = 4Fl^3/3\pi Y(r_2^2 - r_1^2)\cos\theta. \quad (8)$$

Here l is the length of the capillary, r_2 and r_1 are the outer and inner radii of the capillary, θ is the angle of inclination of the spiral from the horizontal plane, and Y is Young's modulus. If the applied field is B_0 and the fields at the ends of the sample chamber are $B_0 + \Delta B_2$ and $B_0 + \Delta B_1$, Eq. (3) gives for the force attributable to the sample,

$$F_s = \frac{\chi_s A_s}{2\mu_0}[B_0(\Delta B_2 - \Delta B_1) + \tfrac{1}{2}(\Delta B_2)^2 - \tfrac{1}{2}(\Delta B_1)^2]. \quad (9)$$

An increased separation Δx of the capacitance plates will result in a change in capacitance, ΔC, equal to

$$\Delta C = -\epsilon_0 \pi R_0^2 \Delta x/d^2 = -C^2 \Delta x/\epsilon_0 \pi R_0^2, \quad (10)$$

where d is the separation and R_0 is the radius of the capacitor plates. Combining Eqs. (8)–(10), we obtain ΔC as a function of χ_s, B_0, and the other parameters of the instrument:

$$\Delta C = -\left(\frac{4}{3\pi\epsilon_0\mu_0 Y}\right)\frac{C^2 l^3 R_i^2}{(r_2^4 - r_1^4)R_0^2} \times \chi_s[B_0(\Delta B_2 - \Delta B_1) + \tfrac{1}{2}(\Delta B_2)^2 - \tfrac{1}{2}(\Delta B_1^2)]. \quad (11)$$

For fused quartz, $Y = 7.2\times10^{10}$ N/m^2 and $4/3\pi\epsilon_0\mu_0 Y = 5.3\times10^5$ in mks units. R_i is the inner radius of the tube containing the sample; ΔB_2 and ΔB_1 can be calculated with reasonable accuracy from Eq. (4) or in this case read from Fig. 1.

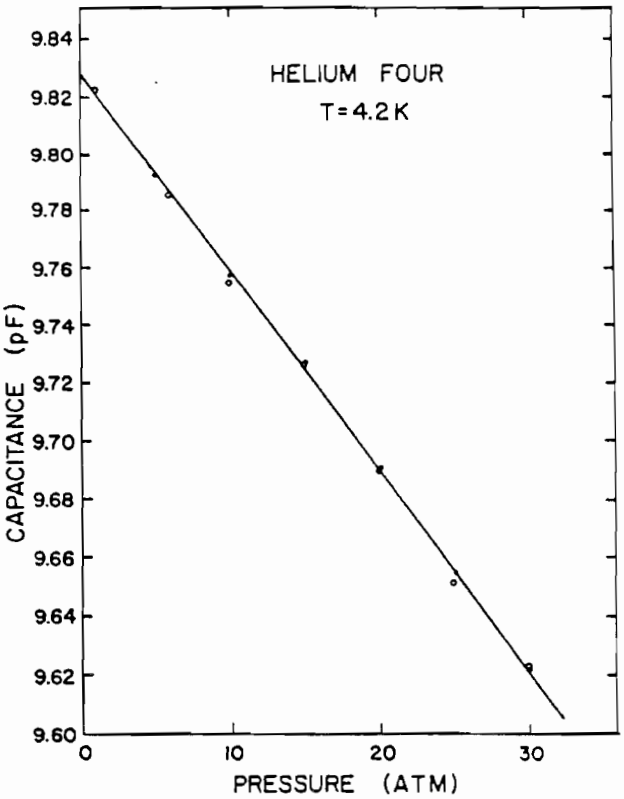

FIG. 4. Response of the apparatus at zero field under increasing pressure of ^{4}He in sample chamber.

III. RESULTS

Our present apparatus allows us to study helium samples in pressures up to the solidification pressure in magnetic fields as great as 19 T and at temperatures down to 1.2 K. It is important to realize that the apparatus as designed will respond to variations in pressure in a manner similar to a Bourdon tube. We show in Fig. 4 the response of the apparatus to an externally applied pressure. This feature allows the continuous monitoring of the pressure in the experimental cell. This is particularly useful when the helium in the fill capillary freezes and external communication via the pressure is lost.

Figure 5 shows the response of the instrument when empty and when filled with liquid ^{4}He in a magnetic field up to 8 T. The initial structure in the change of capacitance corresponds to the region in which the iron cylinder is being magnetized and cannot be described by Eq. (9). For $B_0 > 2.5$ T the iron is approaching saturation and Eq. (9) should apply with increasing accuracy. Figure 5 shows that the change in capacitance corresponding to the liquid ^{4}He for $B_0 > 2.5$ T is negative, as expected for a diamagnetic liquid, and approximately linear. The value of $-\Delta C$ as a function of B_0 agrees with that calculated from Eq. (11) within 15% which is about the accuracy expected from the total uncertainty of the quantities in Eq. (11). Changing the position of the instrument along the axis of the magnet increased the background signal (which was mainly quadratic in B_0). However, the signal from the ^{4}He remained nearly linear in B_0 in fields up to 15 T. Although Eq. (11) could be used to calculate the absolute sensitivity of the apparatus the most practical way to calibrate the apparatus is to determine the response with a well-known substance, in this case liquid ^{4}He.

With ^{3}He the equilibrium response of the apparatus to an applied magnetic field is similar to that observed with ^{4}He when changes in density and total susceptibility are allowed

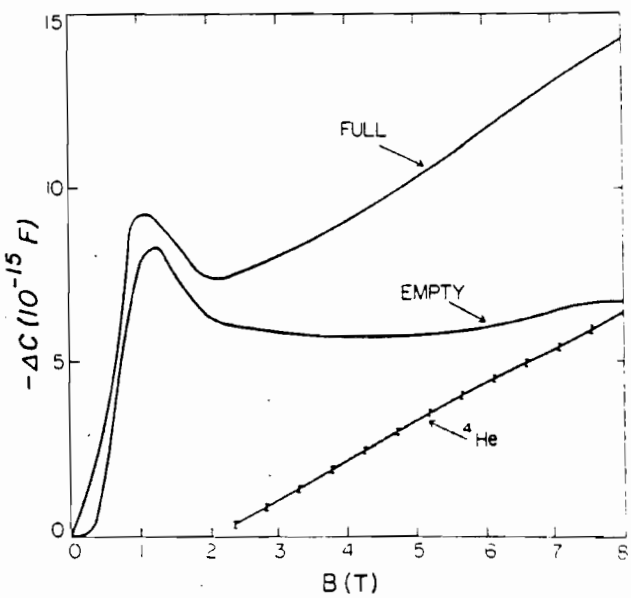

FIG. 5. Measured capacitance decrease $-\Delta C$ as a function of magnetic field B_0 for the sample cell empty and filled with liquid ^{4}He. The difference which is attributable to the helium is also shown.

for. Of special interest is the nonequilibrium response which arises from the long relaxation time of the ^{3}He nuclear susceptibility.[5,6] The susceptibility of liquid ^{3}He can be written as the sum of a diamagnetic term attributable to the atomic electrons (similar to that of ^{4}He and a paramagnetic term attributable to the nuclear magnetic moment. In the temperature region from 0.5 to 3 K the nuclear term is well approximated by Curie's law, so that the total equilibrium susceptibility can be written as

$$\chi = \chi_a + \chi_n \simeq -5.6\times 10^{-7} + \frac{0.42}{T}(10^{-7})\ \text{emu/g}. \tag{12}$$

Since liquid ^{3}He becomes degenerate below the Fermi temperature ($\simeq$0.5 K), Eq. (10) is invalid at lower temperatures and the nuclear term approaches a constant. As a result χ is negative at all temperatures. With a sudden change in field, χ_a attains equilibrium on an atomic time scale, whereas χ_n attains equilibrium much more slowly. The so-called spin-lattice relaxation time T_1 is typically at least hundreds of seconds,[5,6] depends strongly on temperature,[7] and is sensitive to the liquid–container interface.[8]

To measure T_1 in ^{3}He, we have rapidly changed the magnitude of the applied magnetic field and have observed the response of the ^{3}He with time. This method is illustrated in Fig. 6. After a sudden increase in magnetic field from 0 to 12 T in two minutes, there is an immediate decrease in capacitance caused by the atomic diamagnetism. Then, as the nuclear paramagnetism builds up to equilibrium, there is an increase in capacitance whose magnitude decays exponentially to the equilibrium response. This behavior is shown in the upper trace in Fig. 6. The shape of the initial part of this curve is partly caused by the magnetization of the iron and partly by the background response of the unsymmetrically positioned instrument. By fitting the relaxation curve to an exponential, the original magnitude of the nuclear paramagnetism can be deduced. The lower curve in Fig. 6 shows the resistance of a carbon resistor. There is an initial magnetoresistance effect in the changing field. After the field sweep is stopped, the constant resistance shows that the temperature is constant. Since the value of χ_n is known, this sort of measurement also gives an overall calibration of the instrument. The result is that the minimum detectable change of susceptibility $\Delta\chi \simeq 10^{-12}$/g at 12 T. At high fields the sensitivity is about the same as that of SQUID instruments in lower fields. The present apparatus has the advantage of being useful in the highest attainable fields and insensitive to spatial inhomogeneities and to time-dependent field changes associated with such high-field magnets.

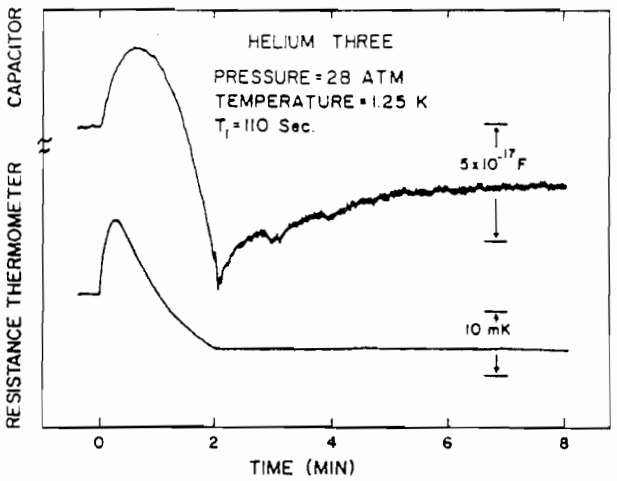

FIG. 6. Sequence of events used to investigate T_1 in ^{3}He. Capacitor: for $t<0$, $H=0$; for $0<t<2$ min, B is swept up to 12 T. (Apparatus position in magnet is responsible for large parabolic response); for $t>2$ min sensitivity is increased by 100 and the nuclear relaxation process is monitored at constant field with time. Resistor: for the same sequence of events, only the magnetoresistance of the resistance thermometer is observed; the temperature remains constant during the relaxation process.

ACKNOWLEDGMENTS

We would like to express our gratitude to Anthony Velluto, Jr., R.V.A. Inc., Woburn, MA, whose patience and expertise were crucial in the construction of the quartz apparatus. This research was supported by the National Science Foundation through grants DMR-8113456 and DMR-8211416.

[1] S. Foner, IEEE Trans. Magn. **MAG-17**, 3358 (1981).
[2] R. Meservey, P. M. Tedrow, J. S. Brooks, and G. O. Zimmerman, J. Appl. Phys. **53**, 2739 (1982).
[3] Since magnetic susceptibility is commonly given in electromagnetic units, we note that one multiplies the value of χ in emu by 4π to obtain χ in rationalized mks units to insert in this expression.
[4] R. M. Bozorth, *Ferromagnetism* (Van Nostrand, New York, 1951), p. 857.
[5] R. H. Romer, Phys. Rev. **117**, 1183 (1960).
[6] J. R. Gaines, K. Luszcynski, and R. E. Norberg, in *Proceedings of the 8th International Conference on Low Temperature Physics*, edited by R. O. Davies (Butterworth, London, 1963), p. 62.
[7] D. Vollhardt and P. Wolfle, Phys. Rev. Lett. **47**, 190 (1981).
[8] J. F. Kelly and R. C. Richardson, in *Low Temperature Physics LT 13* (Plenum, New York, 1974), Vol. I, p. 67.